Vol. 139, No. 1 The American Naturalist January 1992

SPATIAL AGGREGATION AND NEUTRAL MODELS IN FRACTAL LANDSCAPES

BRUCE T. MILNE

Department of Biology, University of New Mexico, Albuquerque, New Mexico 87131

Submitted December 5, 1989; Revised November 19, 1990; Accepted December 12, 1990

Abstract.—Fragmented landscapes alter ecological interactions by modifying the flux of organisms, material, and energy. Fragmented distributions of hypothetical resources and species were represented by several fractal models of landscape patterns at scales ranging from 90 to 2,400 m. Maps of resource aggregations at three scales resulted in multiple-scale notions of "patch," "gap," "edge," "corridor," "source," and "sink." A neutral model of species co-occurrence was developed for analyses conducted at several scales. The neutral model has implications for sampling mutualistic species and for detecting species' responses to changes in environmental conditions. An ecologically meaningful view of landscape pattern depends on the home range size, dispersal ability, or speed with which organisms use resources rather than on the cartographic depiction of the landscape used by humans.

All species are restricted in their ability to occupy space. A long tradition of spatial and temporal analysis has identified several major factors, such as climate and disturbance, that regulate the fragmented distributions of species (see, e.g., Cowles 1899; Warming 1909; Elton 1927; Watt 1947; MacArthur 1972; Walter 1979). Despite the importance of spatial variation in species abundance and resources, the intractable complexity of ecological patterns in space and time prompted early workers to remove ecological interactions from a spatial context and thereby gain an ability to make predictions (Gause 1935; Cole 1954; Bray and Curtis 1957; Hutchinson 1957; Preston 1962; MacArthur and Connell 1966; Whittaker 1967; Margalef 1968; Odum 1971). Subsequent considerations of system stability focused attention once again on the interactions between spatial pattern and dynamics (Bormann and Likens 1979; Shugart and West 1981) and reflected an ongoing concern among ecologists that the central theories of gradients, succession, and competition were incomplete or inadequately tested (Drury and Nisbet 1973; Austin 1985).

Several complementary approaches, including landscape ecology (Forman and Godron 1986), hierarchy theory (Allen and Starr 1982; O'Neill et al. 1986), and supply-side ecology (Gaines and Roughgarden 1985), recently have begun to analyze the origin of fragmented distributions and the mechanisms of species coexistence. Both hierarchy theory and supply-side ecology recognize that ecological processes and patterns are regulated by dynamics occurring simultaneously at several spatial or temporal scales. The return to an explicit spatial context in-

Am. Nat. 1992. Vol. 139, pp. 32–57.

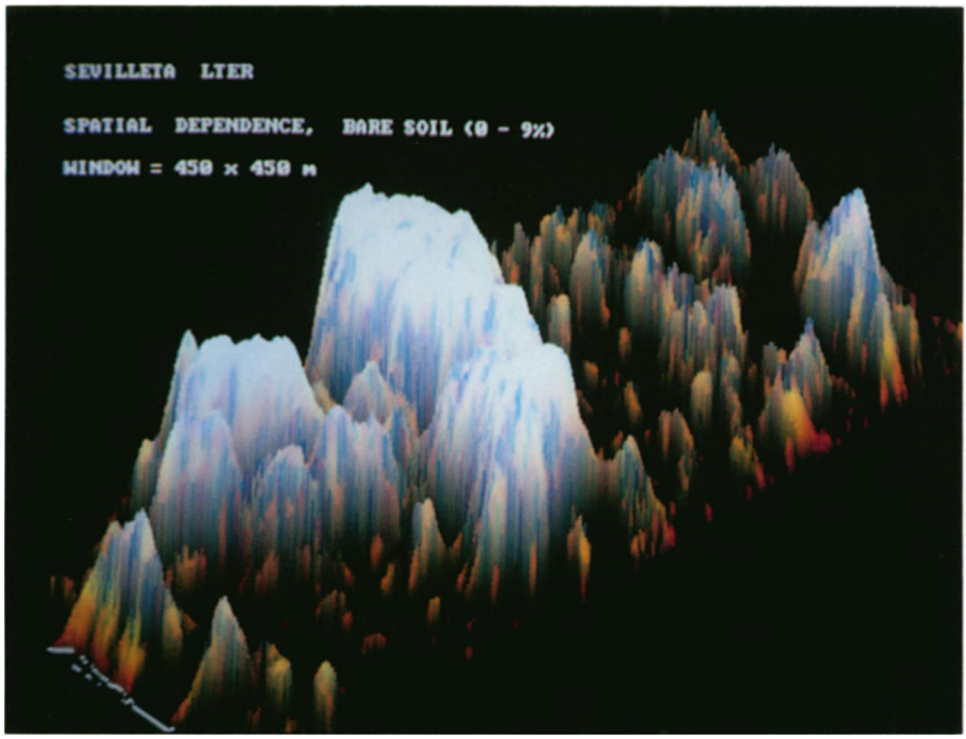

FIG. 7.—Aggregation of the grassland pixels of fig. 2. Surface height is proportional to the number of windows of size $L = 15$ that visited each pixel during the measurement of the probability-density function $p(m,L)$. Coloration corresponds to the frequency of visitation by windows of $L = 3$ (*red*), $L = 9$ (*green*), and $L = 15$ (*blue*). Color intensity was rescaled to relative values. The surface height has been rescaled for clarity at the expense of smoothing the fractal surface ($D = 2.56$).

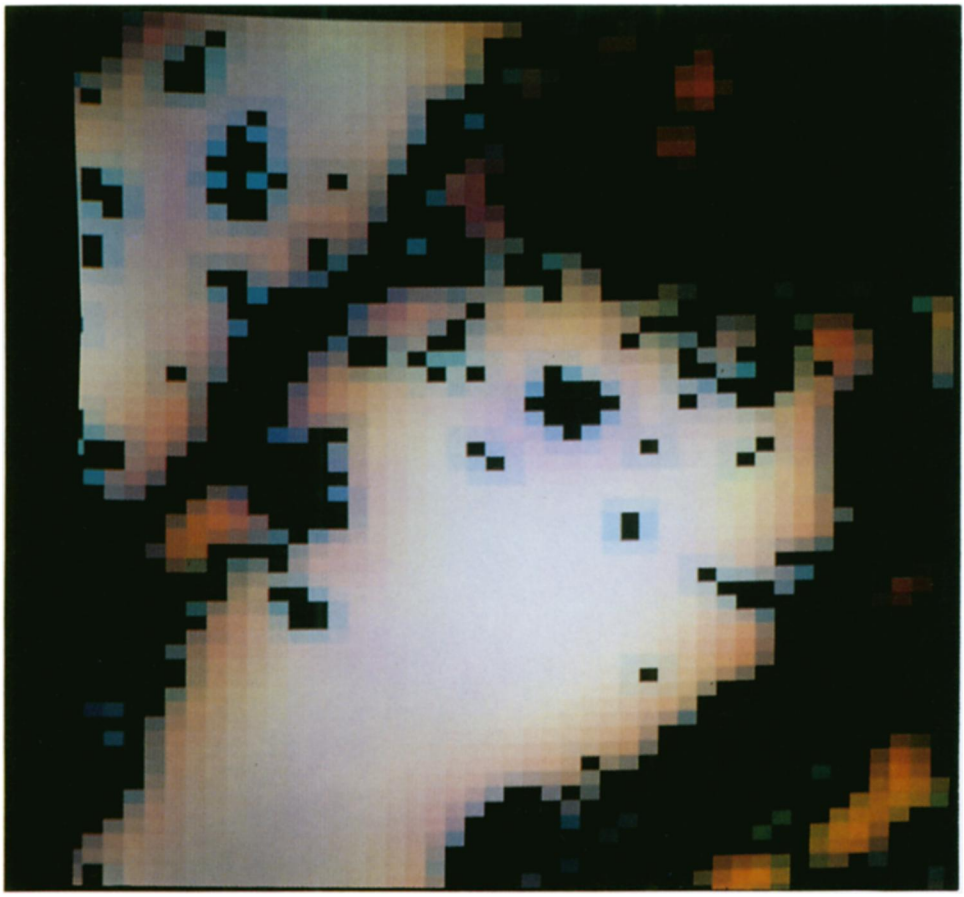

FIG. 8.—Magnification and flat projection of a portion of the aggregation surface. The color scheme is as in fig. 7.

cludes an acute sensitivity to the scale at which observations are made. Scale serves as a particular spatial or temporal perspective applied purposefully by the observer to reveal the differential effects of regulatory or constraining factors. Some factors, such as the influx of larval recruits (Gaines and Roughgarden 1985), are constant over the short term but highly dynamic over broader time scales. Thus, observations made at different scales are informative in the sense that visible and X-ray radiation yield different, but complementary, aesthetic and technical views of a masterpiece painting.

In retrospect, the existing theories of diversity, community composition, succession, and species interactions may be confounded somewhat by the limited ability of theory and empirical work to accommodate the recently discovered consequences of scale (sensu Mandelbrot 1982). The term *scale* has many meanings because any set of observations has both an extent and grain resulting from arbitrary choices made during data collection (O'Neill et al. 1986). Extent (i.e., the spatial and temporal breadth of a set of observations) and grain (i.e., the size of the smallest resolvable unit of observation) interact (Gardner et al. 1987) as two fundamental components of scale. In addition, analytical techniques purposefully impose scales on data such that raw observations are aggregated or pooled within "windows," which thereby provides for the measurement of statistics. Alternatively, pairs of observations at various distances may be compared, as in studies of autocorrelation. Here, in discussions of other studies, *scale* denotes the spatial or temporal extent of a set of observations. Regarding new results presented in this article, *scale* is used in the sense of Mandelbrot (1982) to mean the width of a window and is denoted by L or L', for the length scale. *Scale* in this sense is not the grain of the data, which is presumably fixed. Rather, the grist for the fractal analyses is digital data representing landscape cover types. The data are visualized as pixels on maps or computer monitors. Several pixels may occur simultaneously in sampling units of variable length L.

This article presents a general approach for incorporating a strong sensitivity to scale in a variety of ecological studies. Implications will appear for biological surveys, conservation biology, theories of resource use, sampling strategies, and the interpretation of spatial data, as in geographical information systems. First, however, a brief review of the contributions of landscape ecology, hierarchy theory, and supply-side ecology may indicate why it is necessary to develop tools for relating processes and patterns across a wide range of scales.

SCALE-SENSITIVE STUDIES IN ECOLOGY

A landscape-ecological view of fragmented distributions is explicitly spatial (Forman and Godron 1986; Wiens and Milne 1989) and focuses on the origin and ecological consequences of landscape pattern. For some investigators (e.g., Shugart and West 1981; Delcourt et al. 1982; Urban et al. 1987), landscape patterning results from a combination of temporal and spatial processes spanning from minutes to millennia, from meters to astronomical units. Others (e.g., Neilson and Wullstein 1983; Woodward 1987; Rykiel et al. 1988) emphasize that organisms have scale-dependent responses to constraints, such as moisture avail-

ability or disturbance. Gaines and Roughgarden (1985) emphasize the connection between processes operating at scales outside the ±100-meter-wide purview of classical community ecology (see Ricklefs 1987), for which the term *supply-side ecology* has been coined to represent the role played by distant sources of propagules and predators that modify dispersal rates. Recent studies have addressed spatial heterogeneity by focusing on several scales simultaneously (see Ver Hoef and Glenn-Lewin 1989; Wiens 1989), which adds to earlier observations that correlations among species vary with quadrat size (Noy-Meir and Anderson 1973).

In the hierarchical view, changes in scale reveal factors that appear as constants at some scales and as fluctuations at others (Wiens 1981; Allen and Starr 1982; O'Neill et al. 1986). For example, species exhibit orders of magnitude variation in the scale at which they interact with the environment, as represented by differences in dispersal distances, density, and body length (see, e.g., Morse et al. 1985), correlates of body mass (e.g., range area; see Peters 1983; Brown 1984), and the time required to move about the home range (Swihart et al. 1988). Not only are the distributions of resources and species patchy, ephemeral, or heterogeneous (Erickson 1945), but responses to landscape patterns vary among species due to differences in the scales at which organisms perceive the environment. Temporal effects of scale correspond to thresholds or rates of physiological response (Woodward 1987).

The functional roles of landscape patches (e.g., as sources and sinks; see Pullium 1988) may vary markedly as a consequence of patch mosaic structure (Burel 1989; Milne 1991*a*). Patch mosaic structure is characterized by the kinds, aerial coverages, and juxtapositions of patches. Some mosaics facilitate the flow of disturbance, energy, and resources (Risser et al. 1984; Turner 1987), whereas other arrangements curtail the flows of nutrients such as phosphorus (Correll 1983; Johnston et al. 1988). For deer in New Brunswick, Canada, the juxtaposition of habitat and nonhabitat varies significantly with scale and with the suitability of habitat (Milne et al. 1989). Consequently, the proximity of highly suitable environments to less suitable environments results in a spilling over of animals into the less suitable locations.

In summary, the landscape, hierarchical, and supply-side views of ecology reveal that spatial pattern and the scale of organismal response interact to regulate species distributions. The juxtaposition of resource patches varies through time and with spatial scale (Wiens 1976, 1981; Visscher and Seeley 1982) and regulates processes including dispersal, community interactions, and mass flow of abiotic materials (Gosz et al. 1988). Theoretical, conceptual, and analytical tools are needed for quantifying patch mosaic structure in ways that capture both the statistical aspects of the pattern (see, e.g., Robertson 1987) and the spatial variation of resources, species, and the forces of natural selection.

Three analyses of landscape geometry and resource clustering were developed to determine, first, whether spatial variation in density could be evaluated at many scales while information about local density was simultaneously preserved and, second, whether neutral models could be formulated describing the expected statistical characteristics of species or resources that co-occur at many scales.

Resources generally occur in patches, clusters, or locally dense aggregations. In the first of three analyses, a generally applicable method based on fractal geometry (Mandelbrot 1982) was used to quantify variation in resource density across many scales, for both artificial and remotely sensed grassland patterns.

Second, maps were made to show the spatial distribution of resource aggregations, or clusters, at several scales. The mapping provided a visualization of the physical basis for the statistical scale dependence of landscape pattern. The visualization provided insights about how animals that operate at different scales may perceive variation in resource density. The multiscale analysis revealed that the sizes of resource aggregations vary continuously with scale. Unlike other geostatistical approaches that portray variation as a function of the distance between observations (see, e.g., Robertson 1987; Palmer 1988), maps of aggregation represent the spatial proximity of resources explicitly and obey strict fractal scaling relationships as will be illustrated later. Organisms may respond directly to aggregates of resources while foraging, dispersing, and maintaining territories.

Third, studies of species co-occurrence necessarily include a particular sampling area over which co-occurrence is evaluated. Generally, sampling is conducted at some biologically or methodologically meaningful scale. However, the intuitive notion of scale dependence suggests that greater predictive power might be obtained by studying co-occurrence at many scales simultaneously (see, e.g., Ver Hoef and Glenn-Lewin 1989). Simulated patch mosaics were used to illustrate a scale-sensitive neutral model for the distribution of co-occurring species. The neutral model may help to distinguish arbitrary associations of fractally distributed species from those that are constrained by ecological interactions such as competition. The model has implications for the design of scale-sensitive sampling strategies, source-sink relationships, conservation biology, and biogeography.

METHODS

Study Area

The Sevilleta National Wildlife Refuge and Long Term Ecological Research site (universal transverse Mercator coordinates: zone 13; E 350,000; N 3,805,000) is ≈100,000 ha of semiarid grasslands straddling the Rio Grande and flanked by mountainous areas of *Pinus edulis* and *Juniperus monosperma* woodland at the eastern and western boundaries. The site is located at the confluence of the Great Basin, Great Plains, Chihuahuan, and Mogollon flora (McLaughlin 1986), which contribute over 728 plant taxa to the site (Manthey 1977). Ungrazed by cattle since 1974, the Sevilleta exhibits typical geomorphic and topographical patterns for semiarid grasslands. Granitic and limestone mountains abut alluvial plains and contribute sediment to the bajadas or foot slopes of the mountains. East of the Rio Grande, McKenzie Flats features ephemeral streams called *arroyos* that spill onto the plains from the canyons, carving anastomosing networks into the grassy plains. The plains have deep Turney-Yesum-Wink loamy sand soils and very shallow Nickel-Caliza-Lozier soils (U.S. Department of Agriculture 1988). Soil deposition, erosion, and the complex deposits of variously textured alluvium from

the mountains create natural patterns on the landscape, to which plants respond in both varying species composition and production.

Source of Landscape Data

Remotely sensed data representing complete aerial coverage of an $\approx$18.5-km^2 region of McKenzie Flats and the vicinity were used to investigate the potential consequences of patch mosaic structure at multiple scales. As part of an ongoing study of beetle movements through semiarid grasslands (Wiens and Milne 1989), remotely sensed data were obtained from the Landsat Thematic Mapper (TM) sensor on September 10, 1987, and were used to estimate the coverage of grass and bare soil. I ground-truthed the TM data by estimating the coverage of bare soil along 50-m transects that were approximately the length of the 30-m pixels of the TM imagery (Milne 1991*a*). The transect data were used to calibrate a regression relationship between the percentage of bare soil and TM band 5 (R^2 = 0.86; Milne 1991*a*). The TM band 5, a measure of surface brightness, measures radiance in the short-wave infrared (Goetz et al. 1983). Radiance was coded as digital numbers ranging from 0 to 255, which is the range available in existing digital display hardware.

Classification of the calibrated TM data provided digital maps showing regions occupied by bare soil, the geometry of which affects beetle movements at fine scales (Wiens and Milne 1989). Although several classes of bare soil were calibrated, illustrative analyses of aggregation presented here focused on the spectral class representing 0%–9% bare soil. Grass cover modifies beetle movement (Wiens and Milne 1989), which suggests that the presence of the bare soil class represents an impedance to the dispersal of beetles over distances less than 30 m. Image display, classification, and custom Fortran routines were implemented using the Microimage system from Terra-Mar (Mountain View, Calif.).

Fractal Representations of Landscape Complexity

Much of the complexity apparent in landscapes, resource distributions, and ecosystem heterogeneity can be modeled using fractal geometry (Mandelbrot 1982; Gardner et al. 1987; Krummel et al. 1987; Barnsley 1988; Feder 1988; Milne 1988, 1991*a*, 1991*b*; O'Neill et al. 1988; Voss 1988; De Cola 1989; Gupta and Waymire 1989). Fractals are mathematical representations of complex natural patterns such as clouds, terrain, shorelines, and patch shapes; a technical definition appears in the next paragraph. Like other geostatistical methods, fractal geometry provides measures of spatial dependence at several scales. Fractal analyses are often analogous to, and sometimes directly related to, analyses of autocorrelation and semivariance (see, e.g., Burrough 1981; Palmer 1988). Fractal geometry includes a tremendous diversity of alternative models, all of which share two closely related characteristics.

First, fractals are subsets of the geometrical space within which they reside. Ever since Euclid, points have been envisioned as zero-dimensional objects residing in higher-dimensional sets, such as lines, planes, and solids. In fractal geometry, a collection of points along a line (say, plant intercepts along a transect)

forms a set that occupies less than the entire space that contains the line. Fractals may be described by equations or algorithms that specify the exact portion of the geometrical space the fractal occupies (Barnsley 1988).

Second, by virtue of occupying a small portion of a larger geometrical space, fractals have "fractal dimensions" that are less than or equal to the Euclidean dimension of the space they occupy (Mandelbrot 1982). Thus, very jagged fractal "curves" residing in the two-dimensional plane may have dimensions less than or equal to two. The noninteger values exhibited by fractal dimensions stem from the general scaling law,

$$Q = k L^{D_q}, \tag{1}$$

in which a quantity Q varies as a power of the length scale L (Stanley 1986) and k is a constant. The exponent D_q is the fractal dimension of the quantity, or closely related to the fractal dimension, and quantities that obey this scaling law are fractal (Mandelbrot 1982; Stanley 1986). In general, fractal models provide precise characterizations of complex patterns by representing exponential changes in measured quantities (e.g., perimeter length, semivariance, and area) with changes in length scale. Fractals capture much of the intuitive character of natural heterogeneity and are one of the best available tools for conducting analyses at multiple scales.

As a growing discipline, fractal geometry experiences shifts in emphasis. Early descriptions emphasized the constancy of the fractal dimension across a wide range of scales and the "self-similarity" of geometrical patterns. *Self-similarity* refers to the tendency for small parts of a pattern to resemble the whole pattern, either exactly or statistically (Stanley 1986). The necessity to qualify the precise nature of self-similarity has somewhat reduced the value of the concept, and consequently it will not be emphasized here. A necessary caveat relates to the constancy of a given fractal dimension: a fractal dimension is generally constant within a finite range of length scales and is not a valuable descriptor of patterns at scales outside of the finite range.

The Probability-Density Function

The essence of the fractal analyses presented here involved a particular probability-density function describing the aggregation of points on a map. The probability function has moments, just as the familiar normal distribution has moments (e.g., mean and variance), that vary with the measurement scale. The scaling behavior of the moments is the basis for transforming estimates of mass, area, and density from one scale to another.

The probability-density function $p(m,L)$ is most easily obtained from measurements made on a digital map in raster form, that is, from a computerized map on which each point is addressed using a pair of x and y coordinates. Unlike typical sampling schemes where quadrats are distributed randomly, the density function is generated from square sampling windows that are centered on each pixel representing the land cover type of interest (e.g., grassland). The total number of pixels of the cover type of interest, m, contained in each window of length L is tallied (to center the windows exactly, raster data require that L be an odd number).

Finally, the frequencies for each m value for a given L are determined, and frequency distributions are constructed for a series of different window sizes (Voss 1988; Milne 1991*b*).

Consequently, $N(L)$ is the number of different m values obtained from windows of length L. The frequencies of the m values are transformed to satisfy the probability-density function,

$$\sum_{m=1}^{N(L)} p(m,L) = 1, \tag{2}$$

which indicates that the sum of the probabilities of finding m pixels in a window L units long is 1 (Voss 1988). The quantity $N(L)$ will equal L^2 for maps containing compact patches of at least length L, whereas sparse distributions may yield $N(L) < L^2$. Measurement of $p(m,L)$ provides statistics that describe the aggregation of pixels in the patch mosaic.

The $p(m,L)$ distribution has moments just as the normal distribution has a mean and a variance (Voss 1988; Milne 1991*b*). By definition, the qth moment of $p(m,L)$ is found using the moment-generating function,

$$M(L)^q = \sum_{m=1}^{N(L)} m^q \, p(m,L), \tag{3}$$

where $M(L)^q$ is qth moment obtained using a quadrat L units long: the moment is raised to the qth power. Naturalistic fractals possessing statistical self-similarity with changes in L (Voss 1988) exhibit striking regularity in the qth root of the qth moment as a function of L. In particular, the roots scale as a power of the length scale according to

$$\langle M(L)^q \rangle^{1/q} = k \, L^{D_q}, \tag{4}$$

where the exponent D_q is the fractal dimension of the mapped set if $q = 1$ (see eq. [1]). Natural landscapes containing statistically self-similar fractals exhibit consistent changes in D_q calculated for successive moments (Stanley 1986; Mandelbrot 1989). Observed changes in D_q as a function of q (Milne 1991*b*) probably reflect the large number of quasi-independent processes (see, e.g., Urban et al. 1987) that contribute to landscape patterns.

Nonetheless, when D_q is calculated using the first moment, the dimension is a parameter describing the tendency for patches to be contagious. When $L > 1$ and $D = 2$, the map is filled evenly by the set of interest (i.e., the expected number of pixels in a window of size L is proportional to L^2) or the points are randomly distributed. Fragmented distributions may have $D < 2$ because they fill less than the complete plane at all scales and are aggregated more than random patterns of comparable density. Thus, the fractal dimension relates the expected number or "mass" of pixels (e.g., resources, individuals) observed at one scale to the observations obtained at another scale.

Despite the attention given to fractal dimensions per se, it is equally important to interpret the coefficient on the right-hand side of equation (4). The coefficient

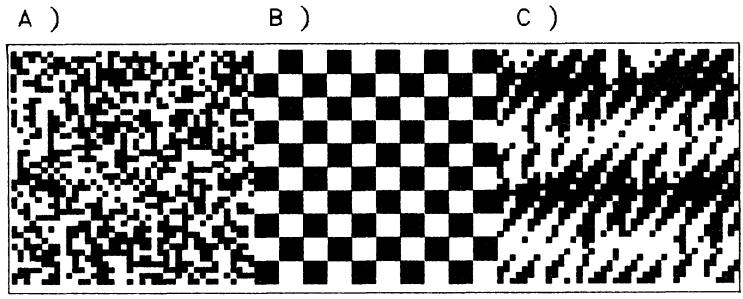

FIG. 1.—Artificial landscape patterns: (*A*) random, (*B*) checkerboard, (*C*) sinusoidal. Each 40 × 40-pixel pattern is 50% covered with filled pixels.

k relates to the sheer preponderance of the pattern relative to the extent of the map within which it occurs. Thus, there is always the possibility that a pattern with a small value for k may exhibit a high fractal dimension, which indicates a relatively compact pattern occupying a small portion of the entire study region. Conversely, k may be large and D small, which indicates a highly dispersed pattern spanning a majority of the study area. Interplay between k and D is very important relative to attempts to extrapolate quantities across scales, although the topic of scale extrapolation is beyond the scope of this article.

Three analyses based on fractal distributions were made to quantify the fractal geometry of patch mosaics, to provide maps of spatial aggregations at several scales simultaneously, and to specify the geometry of overlapping distributions to produce neutral models of species co-occurrence at many scales.

1. *Mosaic structure at multiple scales.*—The analyses of the fractal geometry of a patch mosaic included three phases. To provide some background reference, three maps (i.e., lattices composed of 40 × 40 grid cells) of simulated mosaic patterns were generated, including a random map, a checkerboard, and a sine-wave pattern (fig. 1). Fifty percent of each map was occupied by filled pixels, which are referred to simply as "pixels." White regions of figures 1 and 2 were ignored because they did not represent locations of interest in this study. Four $p(m,L)$ distributions were measured for each simulated map using windows that were 5, 11, 17, and 25 pixels wide. Second, $p(m,L)$ distributions were measured for the map of 0%–9% bare soil generated from the Landsat TM data of the Sevilleta (fig. 2). Window lengths included 5, 7, 9, 11, 17, 23, and 25 pixels, that is, ≈150, 210, 270, 330, 510, 690, and 750 m, respectively. The first moments of each distribution were formed (eq. [3]), logarithmically transformed, and then regressed against the logarithm of L. The fractal dimension of the grassland mosaic was estimated from the slope of the regression. Third, a random map with the same number of pixels and covering the same area as figure 2 was generated as a neutral model (Gardner et al. 1987); that is, pixels were placed at points whose coordinates were obtained from a uniform random distribution. The probabilities $p(m,L)$ for windows of 17 pixels in length were measured on the random and observed maps. Graphical comparison was made between the $p(m,L)$ distributions from the two maps.

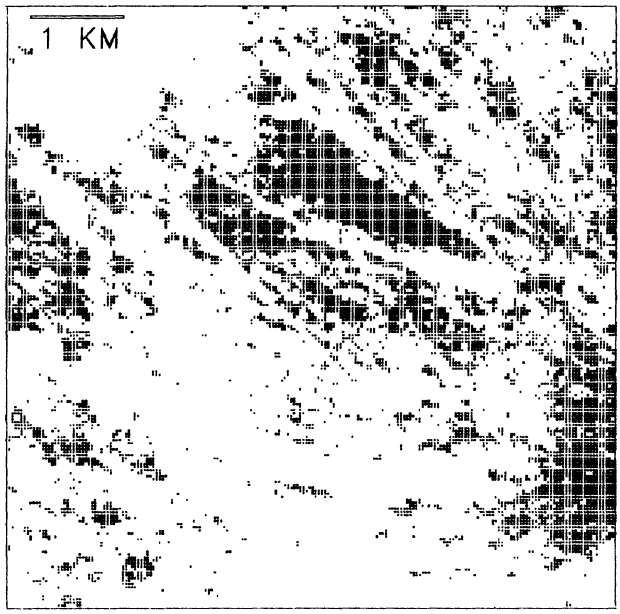

FIG. 2.—Remotely sensed grassland pattern from the Sevilleta National Wildlife Refuge, New Mexico. The 200 × 200-pixel image is composed of 30 × 30-m pixels within which the coverage of bare soil was estimated to range from 0% to 9%.

2. *Aggregation at multiple scales.*—Maps showing the aggregation of grassland pixels were produced by a slight modification of the $p(m,L)$ method. Rather than tallying the number of *pixels* within a window, I tallied the number of *windows* of size L that included each pixel and stored it at the pixel location. Displayed in a spatial context, the counts of window visits created surfaces that were interpreted as measures of the aggregation of grassland pixels. Three surfaces were constructed using windows of $L = 3$, 9, and 15 pixels, corresponding to 90, 270, and 450 m, respectively. Differences between the surfaces were emphasized by displaying the surfaces simultaneously in the red, green, and blue color guns of a computer monitor. The brightness of light in each color gun was proportional to the height of the surface. Although it is possible to compute the number of visits by windows with $L > 15$, 15 is approximately the number of visits that can be displayed by existing image hardware without the added step of rescaling the counts to fall in the range of 0–255.

Aggregation surfaces created with different window sizes could differ simply because small windows yield exponentially fewer visits and, consequently, flatter surfaces or dimmer images. However, when the height of each surface relative to the maximum number of visits observed is rescaled, the relative aggregation of pixels apparent to species operating at different scales is made visible. Interested readers are referred to Meakin (1988) for a discussion of how, in general, the activity of imposing a process on a fractal yields a measure that is itself fractal.

At first, the aggregation maps may seem simply to be a form of "smoothing" at different scales. For the trivial reason that the original grassland map was binary, the counts of windows that visited each pixel were not a smoothed representation of the grassland pixels. Rather, it is ecologically more informative to interpret the counts of window visits as measures of the density of grassland pixels surrounding each grassland pixel. The various window sizes were analogous to the home range sizes used by organisms of increasing mass (Peters 1983; Milne et al., in press) or perhaps the visitation radii used by different pollinators. Thus, inspection of the aggregation map for each of several scales indicates where species with different home range sizes would have to center their ranges to sample a given density of resources.

The scale-dependent characteristics of each surface were studied using methods suggested by Hurst et al. (1965) and discussed by Voss (1988). Unlike fractal patch mosaics, surfaces describing a dependent variable as functions of latitude and longitude may not exhibit fractal scaling quite as described by equation (1). Rather, the dependent variable may vary more strongly as a function of one variable than another. By definition, such a surface is an "affine transformation" of the independent axes, and each point x on the surface can be envisioned as having coordinates $(r_1x, r_2y, \ldots, r_mz)$ where the various coefficients r_i are possibly unique or unequal (Feder 1988). For example, an increment of five units on an independent axis may correspond to a greater or lesser increment on the dependent axis. In contrast, fractal patterns from remotely sensed images of grassland mosaics reside in a coordinate system composed only of latitude and longitude, for which one assumes the axes to be similar.

For some fractal surfaces, the property of self-affinity may hold, for which the mean standardized range of the dependent variable increases as a power of the length scale L' of the independent variables (see, e.g., Feder 1988) used to measure the range (i.e., range = maximum elevation in a window minus the minimum elevation in the same window of length L'). By convention, the scaling exponent is denoted H (after Hurst) and is related to the fractal dimension of the surface by $D = 3 - H$ (Mandelbrot 1982). Surfaces describing generalized regional variables as functions of geographical coordinates may have values of the fractal dimension ranging from two (flat) to nearly three (extremely jagged and tending to fill the three-dimensional space completely). In practice, H and D were obtained after rescaling (Hurst et al. 1965) the range of the dependent and independent variables to an equal range before conducting the analysis.

Mandelbrot (1982) discusses the expectations for fractal dimensions of surfaces relative to models of fractional Brownian motion. Surfaces having $H = 0.5$ may be produced by classical Brownian motion, which exhibits equal probabilities of increases or decreases in values of a dependent variable sampled from a Gaussian distribution (i.e., there are random fluctuations up and down). Values of $H < 0.5$ indicate that the function approaches white noise, whereas $H > 0.5$ indicates high amounts of autocorrelation in the dependent variable. Milne (1991*b*) illustrates changes in H that are interpreted in light of topographical constraints regulating spatial autocorrelation in remotely sensed data from the Sevilleta.

3. *Overlapping mosaics.*—To study the fractal scaling of overlapping mosaics,

the calibrated TM band 5 data were used to create hypothetical spatial patterns analogous to distributions of "species" or resources. The distributions were produced by classifying TM band 5 data into three spectrally overlapping classes (class 1 = TM digital number 65–100, class 2 = 90–120, class 3 = 95–135, inclusive). Thus, pixels with TM band 5 values from 90–100 were members of both classes 1 and 2, and pixels with values of 95–100 were members of classes 1, 2, and 3. The overlapping mosaics provided data analogous to those collected during faunal or floristic surveys in which each sampling point in a grid may contain one or more species.

Although $p(m,L)$ could have been used to estimate the fractal dimension of each class, an alternative method that yields the so-called grid dimension (Voss 1988) was used. The grid procedure represented the typical use of quadrats, in that each cell was placed without regard to the location of particular mosaic pixels. To calculate the grid dimension, a lattice of square grid cells was superimposed on maps of classes 1, 2, and 3, and the number of cells containing any portion of the classes was counted for grid cells of width L = 5, 8, 10, 16, 20, 40, and 80 pixels. Hypothetically, the number of cells occupied by the mosaic decreases according to the equation

$$N(L) = C\,L^{-D_g}, \tag{5}$$

where $N(L)$ is the number of occupied cells of size L and D_g is the grid fractal dimension of the mosaic. Given that there were E = 400 pixels along one edge of the map, the proportion of total grid cells occupied varied as

$$\text{prop}(L) = \frac{C\,L^{-D_g}}{(E/L)^2}, \tag{6}$$

where the denominator is the number of cells of size L^2 over the entire map.

A neutral model of the co-occurrence of classes 1 and 2 was constructed based on the proportion of the landscape occupied by each class. The proportion of the map occupied by classes that occur everywhere and at all scales would simply be prop(L) = 1. However, the proportion of the landscape occupied by S independently distributed classes is

$$A(L) = \prod_{i=1}^{S} \frac{C_i L^{-D(i)_g}}{B\,L^2}, \tag{7}$$

where the numerator describes the amount of landscape covered by the ith class, $D(i)_g$ is the grid fractal dimension of the ith species, the denominator represents area, and B is a constant that varies with the extent of the study. Thus, the product of the ratios across all classes describes the expected proportion of the landscape occupied jointly by the S classes, if one assumes independence in their fractal distributions.

In summary, three measurements of fractal distributions were used to quantify the spatial structure of simulated resource distributions, to formulate neutral models of co-occurring species, and to map the aggregations of resources or species at several scales. The analyses represent the diverse applications that fractals

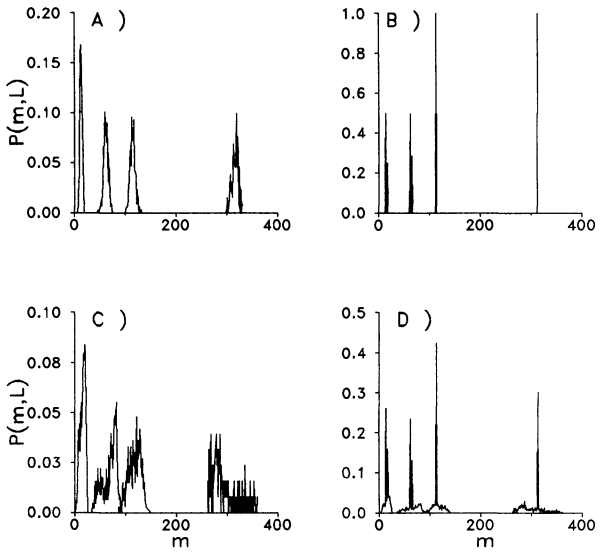

FIG. 3.—Distributions describing the probability of finding m pixels within windows of size L centered on the shaded pixels of fig. 1. Analyses of the (*A*) random pattern, (*B*) checkerboard, (*C*) sinusoidal map, and (*D*) checkerboard and sinusoidal placed side by side. The distributions in each panel were measured, from left to right, in windows of L = 5, 11, 17, and 25, respectively.

have in the study of landscape structure, and they suggest how landscape structure and density vary depending on the scale at which organisms perceive the environment.

RESULTS

Mosaic Structure at Multiple Scales

The $p(m,L)$ distributions obtained from analyses of random, checkerboard, and sinusoidal test patterns revealed striking and interpretable differences between the artificial patterns. The $p(m,L)$ distributions of the random map resembled binomial distributions (fig. 3*A*), with steady increases in the expected value of m as L increased. In contrast, the $p(m,L)$ distributions of the checkerboard pattern (fig. 1*B*) were shaped like spikes, which reflects the monotonic value of $m = \frac{1}{2}L^2$ for large windows (fig. 3*B*). Although little attempt was made to model real landscapes, the patch structure of the sinusoidal pattern was most reminiscent of topographically controlled landscape patterns found in places like Goodland, Kansas (B. T. Milne, personal observation), and yielded $p(m,L)$ distributions of great complexity (fig. 3*C*).

A simulated "ecotone" pattern, composed of the checkerboard and sinusoidal patterns placed side by side (fig. 1*B* and 1*C*), provided $p(m,L)$ distributions that were additive mixtures of the distributions in figure 3*B* and 3*C*. The $p(m,L)$ distributions of figure 3*C* reappeared in figure 3*D*, albeit rescaled and pierced by the

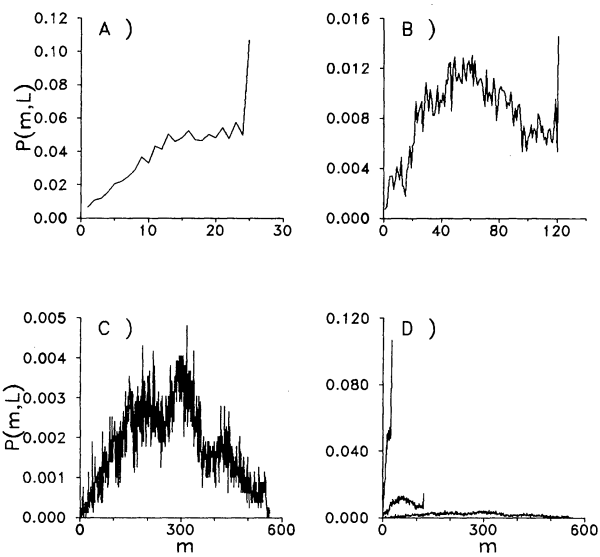

FIG. 4.—Distributions of the probability of finding m pixels within windows of size L on the grassland map of fig. 2. (*A*) window size $L = 5$, (*B*) $L = 11$, (*C*) $L = 25$, and (*D*) all three distributions.

spikes of figure 3*B*, which thus reflects the joining of the distinctive $p(m,L)$ distributions of the checkerboard and sinusoidal patterns. In general, irregular patterns produced $p(m,L)$ distributions that increased in complexity as the window size increased.

Striking patterns of scale dependence were indicated by the shapes of the $p(m,L)$ probability-density functions (fig. 4) of the grassland mosaic (fig. 2). Sampling the map with small 5 × 5-pixel windows (≈150 × 150 m) produced a relatively smooth curve for $p(m,L)$. Increases in L resulted in very complex distributions (e.g., fig. 4*C*). When compared on the same axes (fig. 4*D*), $p(m,L)$ for small windows (i.e., $L = 5$) increased sharply with a maximum $p(m,L)$ at $m = L^2$. The terminal spike indicated that it was most common for the windows to be saturated by pixels. However, with increasing window sizes (i.e., $L = 25$), the maximum value of $p(m,L)$ shifted downward, away from $m = L^2$. Thus, many large windows were not saturated with pixels because large windows were generally longer than the width of grassland patches.

Despite the great variation among the curves, the first moments increased as a power of the length scale used in the analysis (fig. 5). The regression of the logarithmically transformed first moment with the logarithm of L produced an estimate of the fractal dimension of the map ($D = 1.751$, SE = 0.001) and a model of the expected number of pixels as a function of window size ($M^1 = 0.967\ L^{1.751}$). Thus, the map exhibited scale dependence in the expected number of pixels observed in variously sized windows. The extremely high fit of the regression could be attributed to the strong scale dependence of the pattern, the lack of independence among the observations, or both. Thus, a probability value de-

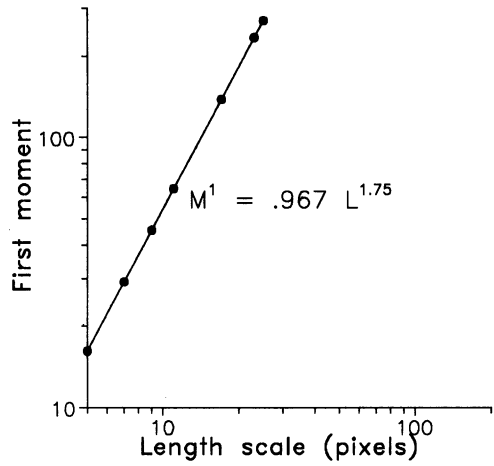

FIG. 5.—The first moments of several probability-density functions obtained from analyses of the Sevilleta grassland pattern. The slope equals the fractal dimension of the grassland pattern.

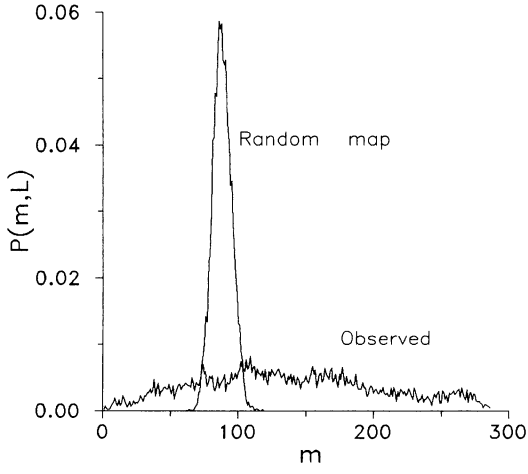

FIG. 6.—Comparison of the probability-density functions obtained from the grassland map with a window size of $L = 17$ and from an analysis of a random map of equal area and density.

scribing the likelihood that the slope of the curve is "significantly different from zero" is not reported, as such a test would violate an assumption of linear regression.

Finally, to determine how the structure of the grassland mosaic differed from random, I measured $p(m,L)$ on a random map of the same extent and number of pixels as figure 2. The empirical grassland map exhibited a much greater diversity of m values (fig. 6), a greater mean and variance, and generally lower probabilities

for many values of m. The grassland $p(m,L)$ indicated a greater diversity of pixel arrangements and clusters compared to a random map of the same overall density.

Aggregation at Multiple Scales

An image was made to represent the scale-dependent clustering of bare soil (fig. 7; See p. 33). The number of windows of size L that included each grassland pixel provided a measure of the aggregation of bare soil. The three aggregation surfaces obtained using windows of length $L = 3$, 9, and 15 pixels were rescaled relative to L^2 and then displayed simultaneously in the red, green, and blue color guns, respectively, of the imaging system (fig. 7). Consequently, white regions had maximal concentrations of pixels at all scales. Pixels with many neighbors were visited by relatively many windows, although the exact meaning of "many neighbors" depended strongly on the window size.

Places with warm or cool hues (fig. 7) represented areas with quite different patterns of pixel aggregation at each scale. For example, magnification of figure 7 revealed both scale-dependent "islands" and gaps in the bare soil mosaic (fig. 8; See p. 34). Isolated reddish areas, such as islands or peninsulas, were visited relatively frequently by small windows but not by large ones. Blue rings surrounding black gaps in the clusters of bare soil indicated that the gaps decreased the apparent aggregation of bare soil observed in small windows but not in large windows (i.e., grassland pixels surrounding the black gaps had relatively many neighbors when large windows were used, and consequently such pixels appeared distinctly blue).

Another common feature of the map was the tendency for white regions to be outlined in red, which indicated that small windows were more sensitive to the edges of the patches. The occurrence of the red edge can be explained by comparing the density of pixels found within 3×3-pixel versus 15×15-pixel windows. The windows yield different densities if one considers windows surrounding a grassland pixel found on a perfectly straight edge of a patch. In such cases, small 3×3 windows would be 66.6% filled (i.e., the area of the window would have two columns, or rows, of grassland pixels, including the filled center column and one filled edge of the window, for a total of $3 \times 2 = 6$ grassland pixels out of a possible 3^2; $6/9 = 66.6\%$). In contrast, the large 15×15-pixel windows would be 53.3% filled with grassland pixels (i.e., $15 \times 8/15^2$). Thus, the large windows yield a dimmer image in the blue color than the small windows yield in red. In all, the relative aggregation, isolation, and perforation of the landscape mosaic differed with the scale used to study aggregation.

Despite the complexity of the surfaces, regular scale-dependent variation in surface elevation was found (table 1). Regressions used to estimate the Hurst parameter of the $L = 3$-pixel surface exhibited strong quadratic departures from the linear model (fig. 9). However, the fit of the Hurst model increased considerably for the $L = 15$-pixel surface (table 1).

Co-occurrence

The fractal grid dimension was used to quantify the scale-dependent mosaic structure of overlapping patch mosaics (table 2). Class 3, with extensive coverage of the map (67.5%), had the highest dimension of 1.98, although the constant of

TABLE 1

HURST MODELS OF THE AGGREGATION SURFACES SHOWN IN FIGURE 7

PARAMETER	SCALE USED TO CREATE THE AGGREGATION SURFACE		
	$L = 3$	$L = 9$	$L = 15$
Constant, C	82.3	43.8	35.2
Exponent (H)	.354	.427	.439
SE of H	.0432	.0317	.0190
Fractal dimension	2.65	2.57	2.56
R^2	.93	.96	.98
Root-mean-squared error	.091	.085	.052

NOTE.—The models are of the form $R = CL'^{H}$, where R is the mean range of the surface elevation observed in a window of size L'. The Hurst exponent H is related to the fractal dimension of the surface by $D = 3 - H$. The best linear fit to the logarithmically transformed Hurst model was obtained for the surface created using windows of $L = 15$, as indicated by a relatively high R^2 and a low root-mean-squared error of the regression model.

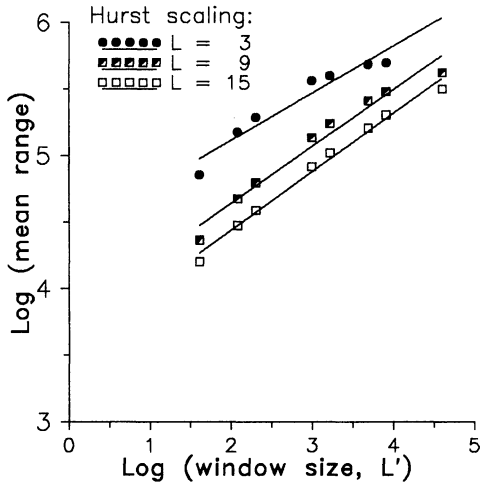

FIG. 9.—Hurst scaling of the mean elevational range of the aggregation surfaces observed within windows of length L'.

equation (5) was a major determinant of the proportion of the landscape occupied by the mosaic (table 2; fig. 10). Despite small numerical differences between the fractal dimensions of the three classes, the exponents had a large effect on the proportion of the landscape occupied at each length scale (fig. 10).

By design, the neutral expectation for the positive co-occurrence of classes 1 and 2 greatly underestimated the actual proportion of the landscape occupied jointly by the classes (fig. 10). The neutral model did not capture the way in which the distribution of the class with minimal coverage (i.e., class 1) constrained the distribution of the intersection of the two classes. The constraining effect of class 1 was indicated by the similarity between the fractal dimensions of class 1 and the dimension of the joint distribution of classes 1 and 2 ($t = -0.197$, $P > .05$).

TABLE 2

FRACTAL SCALING OF CO-OCCURRING PATCH MOSAICS

PARAMETER	CLASS			
	1	2	3	1&2*
Constant, C	44,833	92,679	146,268	39,065
Dimension, D	1.79	1.87	1.98	1.76
SE of D	.009	.014	.006	.014
R^2	.99	.99	.99	.99
Root-mean-squared error	.025	.036	.017	.036

NOTE.—The number of grid cells of area L^2 occupied by each class was modeled as CL^{-D}.
* Class 1&2 is the region of overlap where classes 1 and 2 occurred together.

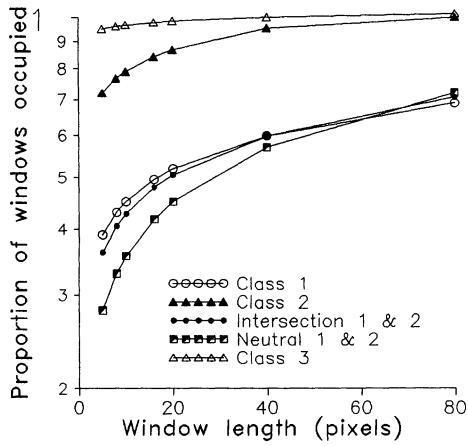

FIG. 10.—Semilogarithmic plot of the predicted occurrence of three simulated landscape classes. Also included are the observed proportions for the intersection of classes 1 and 2 and the neutral expectation for the co-occurrence of classes 1 and 2.

An apparent interaction between the observed and expected distributions of classes 1 and 2 appeared at $L = 80$ (fig. 10). The intersection of the curves for observed and expected proportions at $L \cong 65$ indicated that a neutral model was an effective predictor of species co-occurrence at broad scales but not at fine scales (cf. Getis and Franklin 1987). The critical scale at which a neutral model is sufficient varies with the scaling behavior and dependence between the classes.

DISCUSSION

When viewing maps or satellite images of landscapes, we marvel at the spatial complexity and readily interpret the finest details of the scene. In contrast, earth-bound animals living within home ranges or sibling seeds dispersing away from parent plants effectively integrate landscape pattern at various scales that span several orders of magnitude (see Peters 1983). Consequently, a given landscape

has functionally different geometries depending on the scale of perception. Fractal geometry provides measures of the different geometries and a means of integrating the disparate perceptions of species that occupy a given landscape.

The analyses of aggregation and fractal scaling were based on a probability-density function that is as much at the heart of fractal geometry as the normal distribution is in parametric statistics. Unlike the normal distribution with the associated assumption of independent samples, $p(m,L)$ provides a direct measure of spatial dependence. Natural landscapes are not random (fig. 6; Gardner et al. 1987), so alternatives to the assumptions of parametric statistics are needed for studies conducted in the spatial context (Sokal and Oden 1978; Legendre et al. 1990). In addition, the moments of the probability-density function varied regularly with scale (fig. 5), which suggests a strategy for adjusting measured resource density to match the effective density experienced by species that operate at different scales.

The highly regular increase in the first moment of $p(m,L)$ with scale (fig. 5) offered little for interpreting the physical landscape as organisms may perceive it. Organisms that sample the environment step-by-step or by the mouthful have little ability to integrate information in the way needed to construct $p(m,L)$ and much less the first moment. A fractal dimension of the landscape is a statistical characteristic rather than an observable trait to which organisms may respond directly.

In contrast, the explicit mapping of pixel aggregation (fig. 7) provided a localized view of landscape structure at three scales, much as animals with different home ranges may perceive the landscape. A local view is one that an organism or propagule would experience as it moves from place to place. For example, white regions within figure 7 represented dense aggregations of resources at three scales, and species that use the resources could easily move from one white pixel to an adjacent white pixel because there would be little or no gap in resource availability. Consequently, the contiguous white regions could be true "corridors" for the dispersal of many species, with movement rates being proportional to the local density of resources (i.e., the height of the surface) or some function of density (see Gefen et al. 1983). In contrast, regions with red hues could be dense "patches" for species operating at fine scales but not for broad-scale species. Certainly, broad-scale species could move between small patches, but the utility of sparse resources, relative to the metabolic requirements of massive animals, might be small (Milne et al., in press). The isolation of small patches from the large white patches suggests that they may remain unoccupied by resource users (Milne et al. 1989) because of the large intervening region devoid of resources. Alternatively, vagile species with small home ranges may find the patches readily and thereby avoid competition from broadly ranging species for which the patches are of inconsequential size. The scale-dependent patterns of resource aggregation suggest several effects on species interactions.

Several features of the aggregation map (figs. 7 and 8) suggest extensions of the traditional concepts of "edge," "gap," and "corridor" to the multiscale context (see Forman and Godron 1986 for discussions of these landscape elements). Even though gaps at the northwestern end of the largest patch appeared

distinct (fig. 2), the blue-green shading around the interior edges of gaps, contrasted with the reddish shading at the exterior edge of the patch (fig. 8), indicated that interior and exterior edges (Stanley 1986; Milne 1987) may be differentiated based on the scale-dependent properties of $p(m,L)$. Ecological implications of the interior versus exterior edges relate to the nature of interior and edge species (see, e.g., Forman and Baudry 1984) that perceive the size and arrangement of landscape patches quite differently.

Multiscale notions of "islands," "sources," and "sinks" (sensu Pullium 1988) are equally relevant in considerations of the functional roles of landscape elements. Analyses of landscape structure as a function of scale allow the entire mosaic to be studied simultaneously, which thereby obviates the enumeration of individual islands and the attendant distance effects between all possible pairs of islands.

Rather, fractal aggregations (e.g., fig. 7) indicate that an island is only an island relative to a particular length scale, which may correspond to the dispersal distances used by organisms to hop from one point of land to another. Consequently, an archipelago is also a scale-dependent entity in that some species may infiltrate all points, whereas less vagile species experience greater isolation among points of land. Interactions between the spectrum of dispersal capabilities of a species pool and the fractal geometry of land masses are predicted.

Judging by the degree of fit obtained for the Hurst model of surface roughness, the aggregation map generated by using 15 × 15-pixel windows followed a fractal scaling relationship better than the surface generated from a 3 × 3-pixel window. The quadratic effect observed for small windows should be compared to the tendency for the $p(m,L)$ distributions of small windows to have modal responses at $m = L^2$, whereas large windows do not (fig. 4). In a sense, small windows were easily saturated by bare soil pixels, which made measures of aggregation or the scaling of aggregation somewhat less sensitive to the overall geometry of the pattern. Here, "geometry" could best be characterized by the various moments of the $p(m,L)$ distribution, for both positive and negative values of q (Mandelbrot 1989; Milne et al., in press). The aspects of the pattern that are best characterized by the lower moments will be evident if the windows used in the analysis of aggregation are larger than the average diameter of the patches. Theoretical considerations (see, e.g., Mandelbrot 1989) suggest that there are deeper issues involved with the quadratic departure from the Hurst model than can be treated in this article. Nonetheless, the quadratic departure for small window sizes suggests that windows should be large enough to ensure that the modal value of the $p(m,L)$ distribution is less than the square of L.

The scale dependence of species co-occurrence and the neutral model have implications for sampling and conservation strategies. First, studies of animal-plant interactions, mutualism, and host-parasite relations are probably affected by an interaction between the scale at which samples are collected and the fractal geometry of the species distributions. At sufficiently large scales, co-occurring species may be collected in direct proportion to their abundance predicted by equation (5), whereas at finer scales the rarer of the two species may constrain the number of locations at which the two are found together. Thus, the range of

length scales over which the distribution of one species is dependent on that of the other may be determined by comparing the observed proportion of the landscape occupied to the proportion predicted by the neutral model.

Of course, temporal changes in species occurrence may be detected more readily at high resolution than at coarse resolution. Precisely how high a resolution is sufficient may depend both on the fractal geometry of a species and on the relative fractal dimensions of interacting species. For example, plants tend to form clusters of plants due to birth and death processes and to the dispersal of propagules from nearby parents. Clusters of plants then generate more clusters, in a positive feedback fashion. Consequently, the appearance of new clusters close to old clusters may not signal a fundamental change in the plant population. However, a change that indicates a fundamental change in the dynamics of the population may be the appearance of relatively isolated clusters of plants. For species that are distributed fractally, the meaning of "close to" is relative to the scale of observation, and "close to" can only be defined in a scale-*in*dependent fashion by referring to the fractal dimension. Indeed, the appearance of "isolated" new clusters requires a sensitivity to fractal dimensions. In general, exponentially greater sensitivity to change will be obtained for any given increase in resolution. More to the point, sensitivity to species changes will increase most rapidly with decreases in the length scale for species with low areal or grid fractal dimensions (fig. 10). Perhaps we can best assess temporal changes by observing changes in the scaling behavior of spatial distributions rather than in the distributions per se.

Second, the effect of scale on the co-occurrence of several species is relevant to the design of sustainable nature reserves. Whenever two or more species are of interest, the minimum expected area over which they co-occur is described by equation (7). However, if the species are mutualistic or if differential responses to climatic fluctuation decrease the density of one species faster than that of a second species, an alternative model may be needed to accommodate either the positive or negative association between species.

A model for the co-occurrence of two fractally distributed species whose distributions are contingent on each other or on a limiting resource requires a modification of equation (7), namely, a conditional form:

$$\text{prop}(L) = \prod_{i=1}^{S} \frac{A_i L^{-D(i)_g}}{B L^2} \mid \min(C_j L^{-D(j)_g}) . \tag{8}$$

Here, the proportion of grid cells occupied by the ith species is measured only within windows occupied by species j (or resource) whose coverage of the landscape at scale L is less than the coverage of any other species (i.e., $\min[C_j L^{-D(j)_g}]$ considered for all species $j = 1, \ldots, S$).

Parameter estimation for equation (8) is necessarily a two-step process. First, the constants C_j and $D(j)_g$ are estimated for each species individually, and the species with minimum coverage (e.g., class 1, fig. 10) is found. The distribution of the species with minimal coverage is treated as a constraint on the distribution of other species and used as a template upon which the distribution of other

species is examined. The fractal scaling of the other species is then measured only within grid cells that contain the template species. The constrained distributions are described by $A_i L^{-D(i)_g}$, where the constant A_i and the fractal dimension $D(i)_g$ are contingent on the underlying distribution $\min(C_j L^{-D(j)_g})$.

Despite this accommodation of mutualism, equation (8) remains a "neutral" model because it specifies the co-occurrence of two or more species, if one assumes that the distribution of one species is simply a subset of the distribution of a second. Other factors, such as an Allee effect (Allee et al. 1949) or a threshold density below which a mutualist could not detect the presence of a host, may alter the observed scaling relative to that predicted by equation (8).

Little is known about how the fractal distribution of individual species changes through time (see Turner et al. 1989*a* and 1989*b* for examples from simulation studies). Theoretically, a cosmopolitan species has a grid dimension ≈ 2 and a large constant in equation (1), whereas geographically restricted species have $D_g < 2$. A reasonable prediction is that unfavorable climatic fluctuations will decrease the fractal grid dimension of sensitive species. Consequently, sensitive species will disappear from the landscape rapidly, with the most apparent changes occurring at fine scales (fig. 10). If whole suites of species or keystone species are the targets of conservation, then the ability of a nature reserve to maintain a particular suite of species will be eroded in direct proportion to the rate at which the fractal dimension of the limiting species decreases through time. Sensitive populations in small reserves will be exponentially more volatile than comparable populations in large reserves. Students of island biogeography will appreciate the implied relationship between the exponentially smaller proportion of the landscape occupied by a species viewed with small window sizes (fig. 10) and the well-known exponential increase in the number of species with island area.

ACKNOWLEDGMENTS

The applications of fractal models to landscapes have flourished following conversations with R. H. Gardner, A. R. Johnson, Y. Marinakis, R. V. O'Neill, M. G. Turner, and J. A. Wiens. T. F. H. Allen, S. Grogan, C. Hatfield, D. L. Marshall, M. Palmer, D. Urban, and an anonymous reviewer made helpful suggestions on early drafts of the manuscript. A. King suggested modeling landscapes as sine waves. The assistance of T. Stans, the U.S. Fish and Wildlife Service, the National Science Foundation (BSR-8806435 and BSR-8614981), and the Department of Energy (DE-FG04-88ER60714) is appreciated. This article is Sevilleta Long Term Ecological Research contribution no. 12.

LITERATURE CITED

Allee, W. C., A. E. Emerson, O. Park, T. Park, and K. P. Schmidt. 1949. Principles of animal ecology. Saunders, Philadelphia.

Allen, T. F. H., and T. B. Starr. 1982. Hierarchy: perspectives for ecological complexity. University of Chicago Press, Chicago.

Austin, M. P. 1985. Continuum concept, ordination methods, and niche theory. Annual Review of Ecology and Systematics 16:39–61.

Barnsley, M. F. 1988. Fractals everywhere. Academic Press, New York.
Bormann, F. H., and G. E. Likens. 1979. Catastrophic disturbance and the steady state in northern hardwood forests. American Scientist 67:660–669.
Bray, J. R., and J. T. Curtis. 1957. An ordination of the upland forest communities of southern Wisconsin. Ecological Monographs 27:325–349.
Brown, J. H. 1984. On the relationship between abundance and distribution of species. American Naturalist 124:255–279.
Burel, F. 1989. Landscape structure effects on carabid beetles spatial patterns in western France. Landscape Ecology 2:215–235.
Burrough, P. A. 1981. Fractal dimensions of landscapes and other environmental data. Nature (London) 294:240–242.
Cole, L. C. 1954. The population consequences of life history phenomena. Quarterly Review of Biology 29:103–137.
Correll, D. L. 1983. N and P in soils and runoff of three coastal plain land uses. Pages 207–224 *in* R. Lowrance, R. Todd, L. Asmussen, and R. Leonards, eds. Nutrient cycling in agricultural ecosystems. University of Georgia Agriculture Experiment Station Special Publication 23.
Cowles, H. C. 1899. The ecological relations of the vegetation of the sand dunes of Lake Michigan. Botanical Gazette 27:95–117.
De Cola, L. 1989. Fractal analysis of a classified Landsat scene. Photogrammetric Engineering and Remote Sensing 55:601–610.
Delcourt, H. R., P. A. Delcourt, and T. Webb III. 1982. Dynamic plant ecology: the spectrum of vegetational change in space and time. Quaternary Science Review 1:53–175.
Drury, W. H., Jr., and I. C. T. Nisbet. 1973. Succession. Journal of the Arnold Arboretum Harvard University 54:331–368.
Elton, C. S. 1927. Animal ecology. Sidgwick & Jackson, London.
Erickson, R. O. 1945. The *Clematis Fremontii* var. *Riehlii* population in the Ozarks. Annals of the Missouri Botanical Garden 32:413–460.
Feder, J. 1988. Fractals. Plenum, New York.
Forman, R. T. T., and J. Baudry. 1984. Hedgerows and hedgerow networks in landscape ecology. Environmental Management 8:495–510.
Forman, R. T. T., and M. Godron. 1986. Landscape ecology. Wiley, New York.
Gaines, S., and J. Roughgarden. 1985. Larval settlement rate: a leading determinant of structure in an ecological community of the marine intertidal zone. Proceedings of the National Academy of Sciences of the USA 82:3707–3711.
Gardner, R. H., B. T. Milne, M. G. Turner, and R. V. O'Neill. 1987. Neutral models for the analysis of broad-scale landscape pattern. Landscape Ecology 1:19–28.
Gause, G. F. 1935. Experimental demonstration of Volterra's periodic oscillations in the numbers of animals. Journal of Experimental Biology 12:44–48.
Gefen, Y., A. Aharony, and S. Alexander. 1983. Anomalous diffusion on percolating clusters. Physical Review Letters 50:77–80.
Getis, A., and J. Franklin. 1987. Second-order neighborhood analysis of mapped point patterns. Ecology 68:473–477.
Goetz, A. F. H., B. N. Rock, and L. C. Rowan. 1983. Remote sensing for exploration: an overview. Economic Geology 78:573–590.
Gosz, J. R., C. N. Dahm, and P. G. Risser. 1988. Long-path FTIR measurement of atmospheric trace gas concentration. Ecology 69:1326–1330.
Gupta, V. K., and E. D. Waymire. 1989. Statistical self-similarity in river networks parameterized by elevation. Water Resources Research 25:463–476.
Hurst, H. E., R. P. Black, and Y. M. Simaika. 1965. Long-term storage: an experimental study. Constable, London.
Hutchinson, G. E. 1957. Concluding remarks. Cold Spring Harbor Symposia on Quantitative Biology 22:415–427.
Johnston, C. A., N. E. Detenbeck, J. P. Bonde, and G. J. Niemi. 1988. Geographic information systems for cumulative impact assessment. Photogrammetric Engineering and Remote Sensing 54:1609–1615.

Krummel, J. R., R. H. Gardner, G. Sugihara, R. V. O'Neill, and P. R. Coleman. 1987. Landscape pattern in a disturbed environment. Oikos 48:321–324.

Legendre, P., N. L. Oden, R. R. Sokal, A. Vaudor, and K. Junhyong. 1990. Approximate analysis of variance of spatially autocorrelated regional data. Journal of Classification 7:53–75.

MacArthur, R. H. 1972. Geographical ecology. Princeton University Press, Princeton, N.J.

MacArthur, R. H., and J. H. Connell. 1966. The biology of populations. Wiley, New York.

Mandelbrot, B. 1982. The fractal geometry of nature. Freeman, New York.

———. 1989. Multifractal measures, especially for the geophysicist. Pure and Applied Geophysics 131:5–42.

Manthey, G. T. 1977. A floristic analysis of the Sevilleta Wildlife Refuge and the Ladron Mountains. Master's thesis. University of New Mexico, Albuquerque.

Margalef, R. 1968. Perspectives in ecological theory. University of Chicago Press, Chicago.

McLaughlin, S. P. 1986. Floristic analysis of the southwestern United States. Great Basin Naturalist 46:46–65.

Meakin, P. 1988. The growth of fractal aggregates and their fractal measures. Pages 335–589 *in* C. Domb and J. L. Lebowitz, eds. Phase transitions and critical phenomena. Academic Press, New York.

Milne, B. T. 1987. Hierarchical landscape structure and the Forest Planning Model: discussant's comments in FORPLAN: an evaluation of a forest planning tool. USDA Forest Service General Technical Report RM-140.

———. 1988. Measuring the fractal geometry of landscapes. Applied Mathematics and Computation 27:67–79.

———. 1991*a*. Heterogeneity as a multi-scale characteristic of landscapes. Pages 69–84 *in* J. Kolasa and W. E. Waters, eds. Ecological heterogeneity. Springer, New York.

———. 1991*b*. Lessons from applying fractal models to landscape patterns. Pages 199–235 *in* M. G. Turner and R. H. Gardner, eds. Quantitative methods in landscape ecology. Springer, New York.

Milne, B. T., K. Johnston, and R. T. T. Forman. 1989. Scale-dependent proximity of wildlife habitat in a spatially-neutral Bayesian model. Landscape Ecology 2:101–110.

Milne, B. T., M. G. Turner, J. A. Wiens, and A. R. Johnson. In press. Interactions between the fractal geometry of landscapes and allometric herbivory. Theoretical Population Biology.

Morse, D. R., J. H. Lawton, M. M. Dodson, and M. H. Williamson. 1985. Fractal dimension of vegetation and the distribution of arthropod body lengths. Nature (London) 314:731–734.

Neilson, R. P., and L. H. Wullstein. Biogeography of two southwest American oaks in relation to atmospheric dynamics. Journal of Biogeography 10:275–297.

Noy-Meir, I., and D. J. Anderson. 1973. Multiple pattern analysis, or multiscale ordination: towards a vegetation hologram? Pages 207–231 *in* G. P. Patil, E. C. Pielou, and W. E. Waters, eds. Many species populations, ecosystems, and systems analysis. Statistical ecology. Vol. 3. Pennsylvania State University Press, University Park.

Odum, E. P. 1971. Fundamentals of ecology. 3d ed. Saunders, Philadelphia.

O'Neill, R. V., D. L. DeAngelis, J. B. Waide, and T. F. H. Allen. 1986. A hierarchical concept of ecosystems. Princeton University Press, Princeton, N.J.

O'Neill, R. V., J. R. Krummel, R. H. Gardner, G. Sugihara, B. Jackson, D. L. DeAngelis, B. T. Milne, M. G. Turner, B. Zygmunt, S. W. Christensen, V. H. Dale, and R. L. Grahm. 1988. Indices of landscape pattern. Landscape Ecology 1:153–162.

Palmer, M. W. 1988. Fractal geometry: a tool for describing spatial patterns of plant communities. Vegetatio 75:91–102.

Peters, R. H. 1983. The ecological implications of body size. Cambridge University Press, New York.

Preston, F. W. 1962. The canonical distribution of commonness and rarity. I. Ecology 43: 185–215.

Pullium, H. R. 1988. Sources, sinks, and population regulation. American Naturalist 132:652–661.

Ricklefs, R. E. 1987. Community diversity: relative roles of local and regional processes. Science (Washington, D.C.) 235:167–171.

Risser, P. G., J. R. Karr, and R. T. T. Forman. 1984. Landscape ecology: directions and approaches. Illinois Natural History Survey Special Publication 2.

Robertson, G. P. 1987. Geostatistics in ecology: interpolating with known variance. Ecology 68:744–748.

Rykiel, E. J., Jr., R. N. Coulson, P. J. H. Sharpe, T. F. H. Allen, and R. O. Flamm. 1988. Disturbance propagation by bark beetles as an episodic landscape phenomenon. Landscape Ecology 1:129–139.

Shugart, H. H., and D. C. West. 1981. Long-term dynamics of forest ecosystems. American Scientist 69:647–652.

Sokal, R. R., and N. L. Oden. 1978. Spatial autocorrelation in biology. I. Methodology. Biological Journal of the Linnean Society 10:199–228.

Stanley, H. E. 1986. Form: an introduction to self-similarity and fractal behavior. Pages 21–53 *in* H. E. Stanley and N. Ostrowski, eds. On growth and form: fractal and non-fractal patterns in physics. Nijhoff, Boston.

Swihart, R. K., N. A. Slade, and B. J. Bergstrom. 1988. Relating body size to the rate of home range use in mammals. Ecology 69:393–399.

Turner, M. G., ed. 1987. Landscape heterogeneity and disturbance. Ecological Studies 64. Springer, New York.

Turner, M. G., R. Costanza, and F. H. Sklar. 1989*a*. Methods to evaluate the performance of spatial simulation models. Ecological Modelling 48:1–18.

Turner, M. G., R. H. Gardner, V. H. Dale, and R. V. O'Neill. 1989*b*. Predicting the spread of disturbance across heterogeneous landscapes. Oikos 55:121–129.

Urban, D. L., R. V. O'Neill, and H. H. Shugart. 1987. Landscape ecology. BioScience 37:119–127.

U.S. Department of Agriculture. 1988. Soil survey of Socorro County area, New Mexico. Government Printing Office, Washington, D.C.

Ver Hoef, J. M., and D. C. Glenn-Lewin. 1989. Multiscale ordination: a method for detecting pattern at several scales. Vegetatio 82:59–67.

Visscher, P. K., and T. D. Seeley. 1982. Foraging strategy of honeybee colonies in a temperate deciduous forest. Ecology 63:1790–1801.

Voss, R. F. 1988. Fractals in nature: from characterization to simulation. Pages 21–70 *in* H.-O. Peitgen and D. Saupe, eds. The science of fractal images. Springer, New York.

Walter, H. 1979. Vegetation of the earth and the ecological systems of the geobiosphere. 2d ed. Springer, New York.

Warming, J. E. B. 1909. Oecology of plants. Oxford University Press, London.

Watt, A. S. 1947. Pattern and process in the plant community. Journal of Ecology 35:1–22.

Whittaker, R. H. 1967. Gradient analysis of vegetation. Biological Review 42:207–264.

Wiens, J. A. 1976. Population responses to patchy environments. Annual Review of Ecology and Systematics 7:81–120.

———. 1981. Single sample surveys of communities: are the revealed patterns real? American Naturalist 117:90–98.

———. 1989. Spatial scaling in ecology. Functional Ecology 3:383–397.

Wiens, J. A., and B. T. Milne. 1989. Scaling of "landscapes" in landscape ecology, or, landscape ecology from a beetle's perspective. Landscape Ecology 3:87–96.

Woodward, F. I. 1987. Climate and plant distribution. Cambridge University Press, New York.

Editor: Mark D. Rausher